Attitude Stabilization of a VTOL Quadrotor Aircraft

Abdelhamid Tayebi and Stephen McGilvray

***Abstract*—In this paper, we propose a new quaternion-based feedback control scheme for exponential attitude stabilization of a four-rotor vertical takeoff and landing aerial robot known as a quadrotor aircraft. The proposed controller is based upon the compensation of the Coriolis and gyroscopic torques and the use of a PD^2 feedback structure, where the proportional action is in terms of the vector quaternion and the two derivative actions are in terms of the airframe angular velocity and the vector quaternion velocity. We also show that the model-independent PD controller, where the proportional action is in terms of the vector-quaternion and the derivative action is in terms of the airframe angular velocity, without compensation of the Coriolis and gyroscopic torques, provides asymptotic stability for our problem. The proposed controller as well as some other controllers have been tested experimentally on a small-scale quadrotor aircraft.**

***Index Terms*—Attitude stabilization, nonlinear control, quadrotor, rigid body in space, vertical takeoff and landing (VTOL) aircraft.**

I. Introduction

UNMANNED vehicles are important when it comes to performing a desired task in a dangerous and/or unaccessible environment. Unmanned indoor and outdoor mobile robots have been successfully used for some decades. More recently, a growing interest in unmanned aerial vehicles (UAVs) has been shown among the research community. Being able to design a vertical takeoff and landing (VTOL)-UAV, which is highly maneuverable and extremely stable, is an important contribution to the field of aerial robotics since potential applications are tremendous (e.g., high buildings and monuments investigation, rescue missions, film making, etc.). In practical applications, the position in space of the UAV is generally controlled by an operator through a remote-control system using a visual feedback from an onboard camera, while the attitude is automatically stabilized via an onboard controller. The attitude controller is an important feature since it allows the vehicle to maintain a desired orientation and, hence, prevents the vehicle from flipping over and crashing when the pilot performs the desired maneuvers.

The attitude control problem of a rigid body has been investigated by several researchers and a wide class of controllers has been proposed (see, for instance, [3], [7], [10], [17], and [19], and the list is not exhaustive). This is a particularly interesting problem in dynamics since the angular velocity of the body cannot be integrated to obtain the attitude of the body [7]. The paper [17] contains an interesting list of references and proposes several control algorithms guaranteeing asymptotic stability and, under certain initial conditions, local exponential stability is shown. Most of the existing attitude controllers in the literature are based upon the use of the quaternion representation to describe the attitude of the body. This particular representation allows avoiding the singularities inherent to the direction cosine matrix obtained from Euler rotations [6], [8]. To the best of our knowledge, most of the proposed controllers in the available literature in this field are tested in simulation. In [12], a complete description of an experimental four-rotor aerial robot has been presented without any experimental results. In [2], a commercially available gyro-stabilized quadrotor (Draganflyer III) has been used to test their controller without bypassing the gyro-stabilization feature.

In this paper, we consider the attitude stabilization problem of the quadrotor aircraft. The dynamical model describing the attitude of the quadrotor aircraft contains an additional gyroscopic term caused by the combination of the rotations of the airframe and the four rotors, as well as four additional equations describing the dynamics of the four rotors. In the case where the gyroscopic term is set to zero, and the airframe torques are taken as the actual control inputs, this dynamical model reduces to the well-known model used in the literature concerning the attitude control of a rigid body. Despite the additional gyroscopic term, we show that the classical model-independent proportional derivative (PD) controller can asymptotically stabilize the attitude of the quadrotor aircraft. Moreover, using a new Lyapunov function, we derive an exponentially stabilizing controller based upon the compensation of the Coriolis and gyroscopic torques and the use of a PD^2 feedback structure, where the proportional action is in terms of the vector-quaternion and the two derivative actions are in terms of the airframe angular velocity and the vector-quaternion velocity. The global exponential stability property of our new controller, due mainly to the introduction of the derivative action in terms of the quaternion vector and the compensation of the Coriolis and gyroscopic torques, offers a great advantage in practical applications in terms of transient performance and disturbance rejection especially for large angles and high-speed maneuvers. The proposed controller as well as some other controllers have been tested experimentally on a small-scale quadrotor aircraft. A preliminary version of this paper has been presented in [16].

II. Mathematical Model

The quadrotor aircraft under consideration consists of a rigid cross frame equipped with four rotors as shown in Fig. 1. The up (down) motion is achieved by increasing (decreasing) the

Manuscript received September 20, 2004; revised February 11, 2005. Manuscript received in final form December 2, 2005. Recommended by Associate Editor C.-Y. Su. This work was supported in part by the Natural Sciences and Engineering Research Council (NSERC) of Canada, in part by the Canada Foundation for Innovation (CFI), and in part by the Ontario Innovation Trust (OIT).

A. Tayebi is with the Department of Electrical Engineering, Lakehead University, Thunder Bay, ON P7B 5E1, Canada (e-mail: atayebi@lakeheadu.ca).

S. McGilvray is with the Department of Electrical and Computer Engineering, University of Western Ontario, London, ON N6A 5B8, Canada (e-mail: smcgilvr@uwo.ca).

Digital Object Identifier 10.1109/TCST.2006.872519

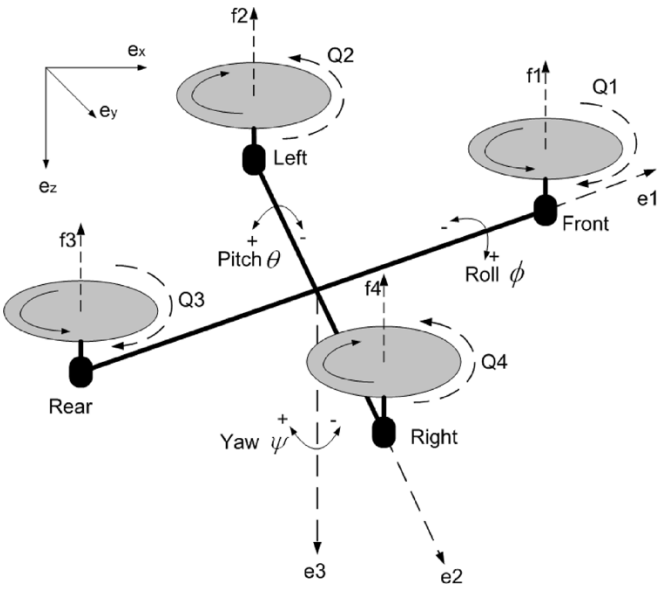

Fig. 1. Quadrotor aircraft.

total thrust while maintaining an equal individual thrust. The forward/backward, left/right and the yaw motions are achieved through a differential control strategy of the thrust generated by each rotor. In order to avoid the yaw drift due to the reactive torques, the quadrotor aircraft is configured such that the set of rotors (right–left) rotates clockwise and the set of rotors (front-rear) rotates counterclockwise. There is no change in the direction of rotation of the rotors (i.e., $\omega_i \geq 0$, $i \in \{1,2,3,4\}$). If a yaw motion is desired, one has to reduce the thrust of one set of rotors and increase the thrust of the other set while maintaining the same total thrust to avoid an up–down motion. Hence, the yaw motion is then realized in the direction of the induced reactive torque. On the other hand, forward (backward) motion is achieved by pitching in the desired direction by increasing the rear (front) rotor thrust and decreasing the front (rear) rotor thrust to maintain the total thrust. Finally, a sideways motion is achieved by rolling in the desired direction by increasing the left (right) rotor thrust and decreasing the right (left) rotor thrust to maintain the total thrust. Let $\mathcal{I} = \{e_x, e_y, e_z\}$ denote an inertial frame, and $\mathcal{A} = \{e_1, e_2, e_3\}$ denote a frame rigidly attached to the aircraft as shown in Fig. 1. The dynamical model described in [4], ignoring aerodynamic effects,[1] with a slight modification of the gyroscopic torques expression due to the fact that the pair of rotors 1–3 rotate in opposite direction of the pair 2–4, is given as follows:

$$\dot{\xi} = v \tag{1}$$

$$\dot{v} = ge_z - \frac{1}{m}TRe_z \tag{2}$$

$$\dot{R} = RS(\Omega) \tag{3}$$

$$I_f\dot{\Omega} = -\Omega \times I_f\Omega - G_a + \tau_a \tag{4}$$

$$I_r\dot{\omega}_i = \tau_i - Q_i, \quad i \in \{1,2,3,4\} \tag{5}$$

where m denotes the mass of the airframe, g denotes the acceleration due to gravity, $e_z = (0,0,1)^T$ denotes the unit vector in the frame $\mathcal{I}$, the vector $\xi = (x,y,z)^T$ denotes the position of the origin of the body-fixed frame $\mathcal{A}$ with respect to the inertial frame $\mathcal{I}$, the vector $v = (v_x, v_y, v_z)^T$ denotes the linear velocity of the origin of $\mathcal{A}$ expressed in $\mathcal{I}$, Ω denotes the angular velocity of the airframe expressed in the body-fixed frame $\mathcal{A}$. The orientation of the airframe is given by the orthogonal rotation matrix $R \in SO(3)$ depending on the three Euler angles ϕ, θ, and ψ denoting, respectively, the roll, the pitch, and the yaw [16]. $I_f \in \mathbb{R}^{3\times 3}$ is a symmetric positive–definite constant inertia matrix of the airframe with respect to the frame $\mathcal{A}$ whose origin is at the center of mass. The speed and moment of inertia of the rotor i are denoted, respectively, by ω_i and I_r. The matrix $S(\Omega)$ is a skew-symmetric matrix such that $S(\Omega)V = \Omega \times V$ for any vector $V \in \mathbb{R}^3$, where $\times$ denotes the vector cross-product.

The reactive torque generated, in free air, by the rotor i due to rotor drag is given by

$$Q_i = \kappa\omega_i^2 \tag{6}$$

and the total thrust generated by the four rotors is given by

$$T = \sum_{i=1}^{4} |f_i| = b\sum_{i=1}^{4} \omega_i^2 \tag{7}$$

where $f_i = -b\omega_i^2 e_3$ is the lift generated by the rotor i in free air (expressed in $\mathcal{A}$), and $\kappa > 0$, $b > 0$ are two parameters depending on the density of air, the size, shape, and pitch angle of the blades, as well as other factors (see [11] and [13] for more details).

The vector G_a contains the gyroscopic torques due to the combination of the rotation of the airframe and the four rotors, and is given by

$$G_a = \sum_{i=1}^{4} I_r(\Omega \times e_z)(-1)^{i+1}\omega_i. \tag{8}$$

The airframe torques generated by the rotors are given by $\tau_a = (\tau_a^1, \tau_a^2, \tau_a^3)^T$, with

$$\begin{aligned} \tau_a^1 &= db(\omega_2^2 - \omega_4^2) \\ \tau_a^2 &= db(\omega_1^2 - \omega_3^2) \\ \tau_a^3 &= \kappa(\omega_1^2 + \omega_3^2 - \omega_2^2 - \omega_4^2) \end{aligned} \tag{9}$$

where d represents the distance from the rotors to the center of mass of the quadrotor aircraft.

Finally, the four control inputs of the system are τ_i, $i \in \{1,2,3,4\}$, which represent the torques produced by the rotors.

Remark 1: Some comparative points with respect to a traditional helicopter can be given as follows: In traditional helicopters, the yaw motion, due to the reactive torque of the main rotor, is compensated by the torque produced by the tail rotor. The energy spent on the tail rotor makes no contribution to the upward thrust of the helicopter. Comparatively, in the quadrotor design, if the four rotors rotate at the same speed, there will be no yaw motion since the reactive torques are cancelled out, as one pair of rotors rotates in the opposite direction of the other pair. In this case, all of the energy spent on the four rotors contributes to generate the upward thrust. The same upward thrust generated by a single rotor in traditional helicopters can be generated by four smaller rotors for the quadrotor; and the fact of using rotors with smaller size helps to reduce the induced mechanical vibrations comparatively to a single large main rotor.

[1]This is justified since our experiment involves a small-scale quadrotor fixed to a ball joint base designed to test the attitude control.

On the other hand, traditional helicopters have somewhat complicated mechanisms for achieving controlled flight, while for the quadrotor, controlled flight is achieved in a quite intuitive manner by differential thrust control of the four rotors as explained in the previous section.

III. Attitude Control Design

In this section, we aim to design a feedback control scheme for the attitude stabilization of the quadrotor aircraft. To this end, we will make use of (3)–(5). Equations (1)–(2) describing the position and the linear velocity of the center of the body-attached frame are not used. Our approach consists of two parts. In the first part, we design the desired airframe torques τ_a for the attitude stabilization. In this part, we present two control schemes; the first one is model dependent and guarantees exponential stability while the second one is model independent but guarantees only asymptotic stability. In the second part, we design the rotor torques required to obtain the desired airframe torques designed in the first part.

One of the drawbacks related to the use of the direction cosine matrix R is the inherent geometric singularity. This drawback can be avoided by using the four-parameter description of the orientation called the quaternion representation [6]–[9], [17], which is based upon the fact that any rotation of a rigid body can by described by a single rotation about a fixed axis [15]. This globally nonsingular representation of the orientation is given by the vector $(q, q_0)^T$ with

$$q = \hat{k}\sin\left(\frac{\gamma}{2}\right), \quad q_0 = \cos\left(\frac{\gamma}{2}\right) \tag{10}$$

where γ is the equivalent rotation angle about the axis described by the unit vector $\hat{k} = (\hat{k}_1, \hat{k}_2, \hat{k}_3)$, subject to the constraint

$$q^T q + q_0^2 = 1. \tag{11}$$

The rotation matrix R is related to the quaternion through the Rodriguez formula [5], [15], and an algorithm for the quaternion extraction is presented in [9]. Although the quaternion representation is nonsingular, it contains a sign ambiguity (i.e., (q, q_0) and $(-q, -q_0)$ lead to the same orientation) which can be resolved by choosing the following differential equations [5], [17]:

$$\begin{aligned} \dot{q} &= \frac{1}{2}(S(q) + q_0 I)\Omega, \\ \dot{q}_0 &= -\frac{1}{2}q^T\Omega \end{aligned} \tag{12}$$

where I is a 3×3 identity matrix.

A. Step 1: Airframe Torques Design

In this part, we consider τ_a as a control input to be designed for the attitude stabilization of the quadrotor aircraft. Without the gyroscopic term, the dynamical model (3)–(4) is similar to the well-known model used in the literature concerning the attitude control of a rigid body. Our objective is to stabilize the equilibrium point $(\phi, \theta, \psi, \Omega) = 0$, or $(R = I, \Omega = 0)$. This can be achieved by the stabilization of the two equilibrium points $(q = 0, q_0 = \pm 1, \Omega = 0)$ for (12) and (4). Since $q_0 = 1$ corresponds to $\gamma = 0$ and $q_0 = -1$ corresponds to $\gamma = 2\pi$, it is clear that $q_0 = \pm 1$ correspond to the same physical point. Hence, the two equilibrium points $(q = 0, q_0 = \pm 1, \Omega = 0)$ are, in reality, a unique physical equilibrium point corresponding to $(R = I, \Omega = 0)$. In the sequel, the Euler angles and the equivalent rotation angle γ are taken between $-\pi$ and π, which imply that $0 \leq q_0 \leq 1$.

Now, one can state the following result:

Theorem 1: consider (3) and (4) under the following control law:

$$\tau_a = \Omega \times I_f\Omega + G_a + I_f\dot{\bar{\Omega}} - \Gamma_2\tilde{\Omega} - \Gamma_3 q, \tag{13}$$

where $\tilde{\Omega} = \Omega - \bar{\Omega}$, $\bar{\Omega} = -\Gamma_1 q$, and $\dot{\bar{\Omega}} = -\Gamma_1\dot{q} = -(1/2)\Gamma_1(q_0 I + S(q))\Omega$, with Γ_1 is a 3×3 symmetric positive definite matrix and

- Γ_2, Γ_3 are 3×3 diagonal positive definite matrices in the case where I_f is diagonal;
- Γ_2 is a 3×3 symmetric positive definite matrix and $\Gamma_3 = \alpha I$, where α is a positive scalar, in the case where I_f is not diagonal.

Then, the equilibrium point $(R = I, \Omega = 0)$ is exponentially stable.

Proof: Let us consider the following Lyapunov function candidate:

$$V = q^T q + (q_0 - 1)^2 + \frac{1}{2}\tilde{\Omega}^T\Gamma_3^{-1}I_f\tilde{\Omega} \tag{14}$$

whose time derivative, in view of (4) and (11)–(13) is given by

$$\dot{V} = -q^T\Gamma_1 q - \tilde{\Omega}^T\Gamma_3^{-1}\Gamma_2\tilde{\Omega} \tag{15}$$

which implies that the state variables of (4) and (12) are bounded and $\lim_{t\to\infty}\tilde{\Omega}(t) = \lim_{t\to\infty} q(t) = 0$. This implies that $\lim_{t\to\infty}\Omega(t) = \lim_{t\to\infty}\bar{\Omega}(t) = 0$. Hence, from (11), one can conclude that $\lim_{t\to\infty} q_0(t) = \pm 1$ (note that $q_0 = -1$ is excluded since the angles are taken such that $0 \leq q_0 \leq 1$).

Now, let us show the exponential stability. From the fact that $0 \leq q_0 \leq 1$ and (11), we have

$$\|q\|^2 = 1 - q_0^2 \geq 1 - q_0. \tag{16}$$

Consequently, V can be bounded from above as follows:

$$V \leq \max\left\{2, \frac{\lambda_{\max}(\Gamma_3^{-1}I_f)}{2}\right\}(\|q\|^2 + \|\tilde{\Omega}\|^2). \tag{17}$$

On the other hand, $\dot{V}$ can be bounded from above as follows:

$$\dot{V} \leq -\min\{\lambda_{\min}(\Gamma_1), \lambda_{\min}(\Gamma_3^{-1}\Gamma_2)\}(\|q\|^2 + \|\tilde{\Omega}\|^2). \tag{18}$$

Hence, from (17) and (18), one can conclude that $\dot{V} \leq -\beta V$, where

$$\beta = \frac{\min\{\lambda_{\min}(\Gamma_1), \lambda_{\min}(\Gamma_3^{-1}\Gamma_2)\}}{\max\{2, 0.5\lambda_{\max}(\Gamma_3^{-1}I_f)\}}$$

with $\lambda_{\min}(\star)$ and $\lambda_{\max}(\star)$ denoting, respectively, the minimum and maximum eigenvalue of $(\star)$. □

Remark 2: If we consider the system such that Ω is sufficiently small and R close to identity, the Coriolis and gyroscopic terms can be neglected in the control law (13) to obtain the following reduced-complexity locally stabilizing controller:

$$\tau_a = I_f\dot{\bar{\Omega}} - \Gamma_2\tilde{\Omega} - \Gamma_3 q. \tag{19}$$

Note that the control law (13) requires the compensation of the Coriolis and gyroscopic torques involving the airframe inertia I_f and the rotor inertia I_r. Now, we will show that the classical PD feedback control without compensation of the Coriolis

and gyroscopic torques (i.e., model-independent control) can asymptotically stabilize the attitude of the quadrotor aircraft.

Theorem 2: Consider (3) and (4) under the following control law:

$$\tau_a = -\Gamma_4 \Omega - \alpha q \tag{20}$$

where Γ_4 is a 3×3 symmetric positive definite matrix and α is a positive parameter. Then, the equilibrium point $(R = I, \Omega = 0)$ is globally asymptotically stable.

Proof: The time derivative of the following Lyapunov function candidate:

$$V = \alpha q^T q + \alpha (q_0 - 1)^2 + \frac{1}{2} \Omega^T I_f \Omega \tag{21}$$

in view of (4), (11), (12), and (20), and using the fact that $\Omega^T(\Omega \times I_f \Omega) = 0$ and $\Omega^T G_a = \Omega^T(\Omega \times e_z) \sum_{i=1}^{4} I_r (-1)^{i+1} \omega_i = 0$, is given by

$$\dot{V} = -\Omega^T \Gamma_4 \Omega \tag{22}$$

which implies that $\Omega(t)$, $q(t)$ and $q_0(t)$ are bounded. Using La Salle's invariance theorem, one can easily show that $\lim_{t \to \infty} \Omega(t) = \lim_{t \to \infty} q(t) = 0$ and $\lim_{t \to \infty} q_0(t) = \pm 1$. Therefore, the equilibrium point $(R = I, \Omega = 0)$ is globally asymptotically stable. □

Remark 3: It is easy to show the following controller with Coriolis and gyroscopic torques compensation:

$$\tau_a = \Omega \times I_f \Omega + G_a - \Gamma_4 \Omega - \bar{\alpha} q \tag{23}$$

with

- Γ_4 and $\bar{\alpha}$ are 3×3 diagonal positive definite matrices in the case where I_f is diagonal;
- Γ_4 is a 3×3 symmetric positive-definite matrix and $\bar{\alpha} = \alpha I$, where α is a positive scalar, in the case where I_f is not diagonal, provides global asymptotic stability for our problem. In fact, in contrast to the control law (20), this controller allows to use a matrix gain for the quaternion feedback.

Remark 4: The control law (13) can be written in the following form:

$$\tau_a = \Omega \times I_f \Omega + G_a - (\Gamma_3 + \Gamma_2 \Gamma_1) q - \Gamma_2 \Omega - I_f \Gamma_1 \dot{q}, \tag{24}$$

which is basically a PD^2 feedback with Coriolis and gyroscopic torques compensation. The two derivative actions are related to the angular velocity (Ω) and the "quaternion velocity" ($\dot{q}$). Note that $\dot{q}$ is obtained explicity from (12). The control law (20) is a classical PD feedback, where the derivative action is related to the angular velocity (Ω). It is similar to the control laws proposed in [7], [10], and [19]. The main advantage of the control law (20) with respect to the control law (13) is the fact that the model parameters are not required and the control law is much simpler to implement. The main advantages of the control law (13) with respect to the control law (20) are:

1) the ability to use a matrix gain Γ_3 instead of a scalar gain in the quaternion feedback;
2) the exponential convergence property mainly due to the compensation of the Coriolis and gyroscopic terms and the use of the vector-quaternion time-derivative $\dot{q}$.

Remark 5: It is worth noting that the set-point regulation problem is implicitly included in the previous results. In fact, if we want to stabilize the quadrotor at an arbitrary configuration, we have to define the error vector as $[\phi - \phi_d, \theta - \theta_d, \psi - \psi_d]^T$ and obtain the corresponding quaternion (q, q_0) to be used in the previous control laws. Note that the desired attitude angles ϕ_d, θ_d, and ψ_d can be specified by the pilot to control the motion of the quadrotor in space.

B. Step 2: Motor Torques Design

In reality, the control inputs in (1)–(5) are the four rotor torques τ_i, $i \in \{1, 2, 3, 4\}$. To design the rotor torques, one has to find the desired speed of each rotor $\omega_{d,i}$, $i \in \{1, 2, 3, 4\}$, corresponding to the desired airframe torques $\tau_a = (\tau_a^1, \tau_a^2, \tau_a^3)^T$ obtained from (13) or (20). To this end, we must specify the desired total thrust T or, for instance, obtain it from the altitude feedback controlling the z-position of the quadrotor aircraft as discussed later in Remark 7. The desired speed for the four motors can be obtained from (7) and (9). That is, $\varpi_d = M^{-1} \mu$, with $\varpi_d = (\omega_{d,1}^2, \omega_{d,2}^2, \omega_{d,3}^2, \omega_{d,4}^2)^T$, $\mu = (\tau_a^1, \tau_a^2, \tau_a^3, T)^T$ and

$$M = \begin{pmatrix} 0 & db & 0 & -db \\ db & 0 & -db & 0 \\ \kappa & -\kappa & \kappa & -\kappa \\ b & b & b & b \end{pmatrix} \tag{25}$$

where M is nonsingular as long as $db\kappa \neq 0$.

Note that in certain cases, some elements of ϖ_d resulting from $M^{-1}\mu$ might be negative, suggesting the reversal of the rotors direction, which is not feasible in our case. This case is not likely to occur if the desired total thrust T is sufficiently large with respect to the required airframe torques.

Now, having $\omega_{d,i}$, $i \in \{1, 2, 3, 4\}$, one can design τ_i as follows:

$$\tau_i = Q_i + I_r \dot{\omega}_{d,i} - k_i \tilde{\omega}_i \tag{26}$$

where k_i, $i \in \{1, 2, 3, 4\}$ are four positive parameters, and $\tilde{\omega}_i = \omega_i - \omega_{d,i}$. In fact, applying (26) to (5) leads to

$$\dot{\tilde{\omega}}_i = -\frac{k_i}{I_r} \tilde{\omega}_i \tag{27}$$

which shows the exponential convergence of ω_i to $\omega_{d,i}$ and, hence, the convergence of the airframe torques to the desired values leading to the attitude stabilization of the quadrotor aircraft.

In our application, the dc motors are voltage controlled, so we need to obtain the voltage input to each motor. Assuming that the motor inductance is small and taking into consideration the gear ratio, one can obtain the voltage to be applied to each motor as follows:

$$v_i = \frac{R_a}{k_m k_g} \tau_i + k_m k_g \omega_i \tag{28}$$

where R_a is the motor resistance, k_m is the motor torque-constant, and k_g is the gear ratio. Since we are using the same motors, all of the parameters are the same for the four motors. Finally, the voltage v_i is used to generate the pulsewidth-modulated (PWM) signal for the control of the motor i.

Intuitively, for better transient performance, one has to ensure that the convergence of ω_i to $\omega_{d,i}$ is faster than the convergence of the attitude to zero. This could be realized by taking

$k_i/I_r > \beta$, where β is defined in the proof of Theorem 1.

Remark 6: In the control law (26), the derivative of the desired rotors speed is required. It is possible to derive the analytical expression for $\dot{\omega}_{d,i}$, using $\varpi_d = M^{-1}\mu$ as follows:

$$\dot{\omega}_d = \frac{1}{2} A_\omega M^{-1} \dot{\mu} \tag{29}$$

where $\dot{\mu} = [\dot{\tau}_a^T, \dot{T}]^T$, $\dot{\omega}_d = (\dot{\omega}_{d,1}, \dot{\omega}_{d,2}, \dot{\omega}_{d,3}, \dot{\omega}_{d,4})^T$, and $A_\omega = diag(1/\omega_{d,1}, 1/\omega_{d,2}, 1/\omega_{d,3}, 1/\omega_{d,4})$. If we consider that the desired total thrust is a constant, and $\omega_{d,i} \neq 0$, one can obtain $\dot{\omega}_{d,i}$ from (29), using $\dot{T} = 0$. The derivative of the desired airframe torque can be obtained explicitly from (13) or (20). For the control law in Theorem 2, one can obtain $\dot{\tau}_a$, using (4), (12), and (20), as follows:

$$\dot{\tau}_a = -\Gamma_3 I_f^{-1}(-\Omega \times I_f \Omega - G_a + \tau_a) - \frac{\alpha}{2}(S(q) + q_0 I)\Omega. \tag{30}$$

However, to simplify our control implementation and avoid the singularity occuring at $\omega_{d,i} = 0$, in our experiments, we will obtain $\dot{\omega}_{d,i}$ from $\omega_{d,i}$ using a filtered derivative also called the "dirty derivative" (i.e., $\dot{\omega}_{d,i} = (s/(1+T_f s))[\omega_{d,i}]$, with $T_f = 1/2\pi f_c$, where f_c is the cutoff frequency).

Remark 7: As stated before, the total thrust T can be designed in order to control the altitude (z-position) of the quadrotor aircraft. Assuming that the z-position is available for feedback, one can use (1) and (2) to design T in order to make the altitude z converge to the desired setpoint z_d. For the sake of simplicity, one can consider the hover (or near to hover) case (i.e., $R \simeq I$). In this case, one can easily design a linear feedback controller using the tools from linear control theory.

Remark 8: In practice, the motion of the quadrotor aircraft in space is achieved by the pilot (onboard or through a remote control) by specifying the desired total thrust, roll, pitch and yaw, while the attitude is automatically controlled according to the algorithms proposed in the previous section. The pilot can also use an automatic altitude controller discussed in Remark 7, in order to hover at a constant desired altitude. In the box "Pilot/Remote control" shown in Fig. 2, an adequate strategy could be implemented to generate the desired attitude angles and the desired total thrust.

IV. Experimental Results

Our experimental quadrotor aircraft is an "in-house" modified version of the Draganflyer III from RC Toys (http://www.rctoys.com). In fact, we kept the airframe, the motors, and the blades of the Draganflyer III and added our own "low-cost" sensors and electronic circuitry. Since, our objective was to safely test our attitude controller, we decided to use a stationary ball joint base, as shown in Fig. 3. This base gives the aircraft unrestricted yaw movement and around $\pm 30°$ of pitch and roll, while restricting the aircraft to a fixed point in the three-dimensional space.

Experimental testing has been performed, with a sampling frequency of 2 kHz, using a dSPACE DS1104 R&D controller board. The dSPACE ControlDesk software in combination with

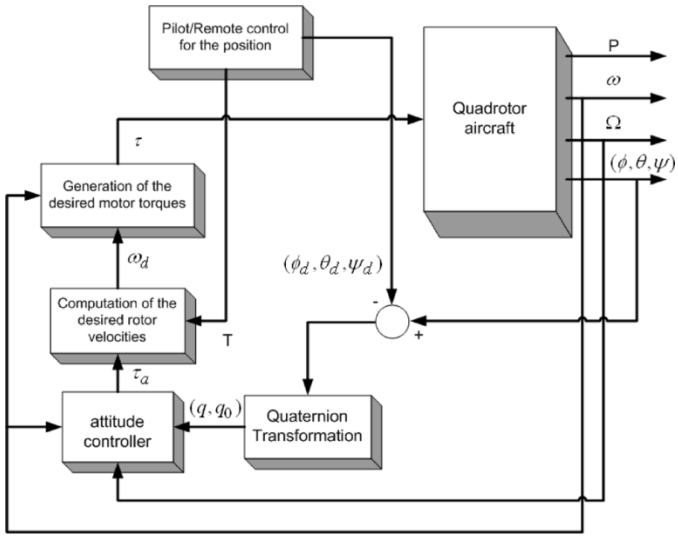

Fig. 2. Control implementation.

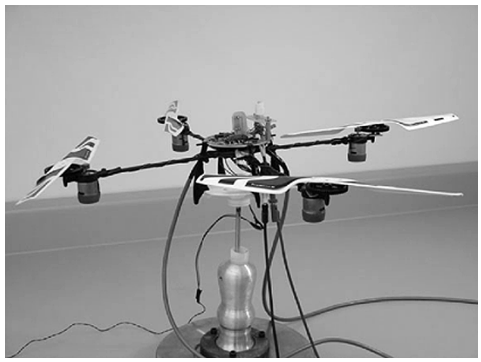

Fig. 3. Quadrotor aircraft experimental setup.

Matlab, Simulink, and Real-Time Workshop allows an easy implementation of the control algorithm in block diagram format via simulink, with real-time adjustments of the control gains.

The four dc permanent-magnet mini motors are geared to each rotor by a speed reduction ratio of 5.6:1. The motors are current amplified with a power metal-oxide semiconductor field-effect transistor and driven by PWM signals.

The rotor velocities $\omega_i, i \in \{1, 2, 3, 4\}$ are obtained from Hall Effect sensors in combination with earth magnets.

The desired acceleration of each rotor $\dot{\omega}_d = (\dot{\omega}_{d,1}, \dot{\omega}_{d,2}, \dot{\omega}_{d,3}, \dot{\omega}_{d,4})^T$ required for the motor torques control design has been obtained by using a filtered derivative of the form $\dot{\omega}_{d,i} = (s/(1+T_f s))[\omega_{d,i}]$ where $T_f = 0.008$ represents a cutoff frequency of 20 Hz. The angular velocity of the aircraft Ω is obtained from three orthogonally mounted gyroscopes. High-frequency noise is sufficiently removed from the Ω measurement by adding first-order low-pass software filters each with a cutoff frequency of 20 Hz.

Attitude estimation of the aircraft has proven to be a challenge. Accurate measurements of the roll, pitch and yaw angles in real-time over a wide range of operating conditions are not easily achieved. Real-time attitude estimation has required fusing measurements from the gyroscopes with measurements

TABLE I
QUADROTOR AIRCRAFT MODEL PRAMETERS

Parameter	Description	Value	Units
g	Gravity	9.81	m/s^2
m	Mass	0.468	kg
d	Distance	0.225	m
I_r	Rotor Inertia	3.4×10^{-5}	$kg \cdot m^2$
I_{f_ϕ}	Roll Inertia	4.9×10^{-3}	$kg \cdot m^2$
I_{f_θ}	Pitch Inertia	4.9×10^{-3}	$kg \cdot m^2$
I_{f_ψ}	Yaw Inertia	8.8×10^{-3}	$kg \cdot m^2$
R_a	Motor Resistance	0.67	Ω
k_m	Motor Constant	4.3×10^{-3}	$N \cdot m/A$
k_g	Gear Ratio	5.6	
b	Proportionality Constant	2.9×10^{-5}	
κ	Proportionality Constant	1.1×10^{-6}	

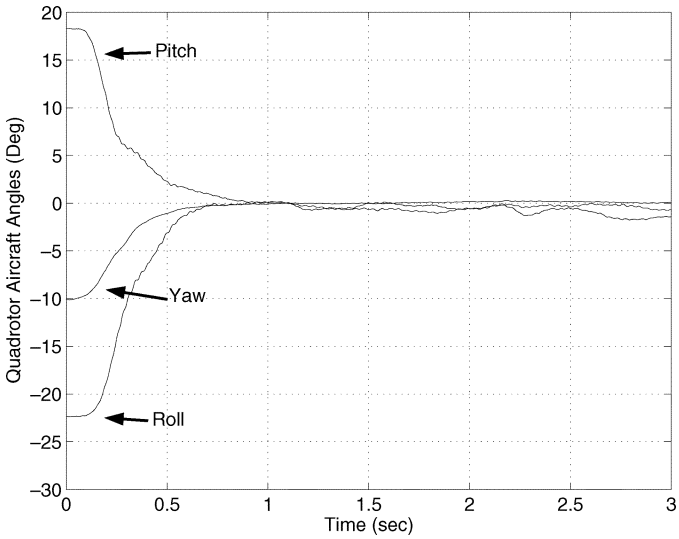

Fig. 4. Aircraft angles, controller (13), Experiment 1.

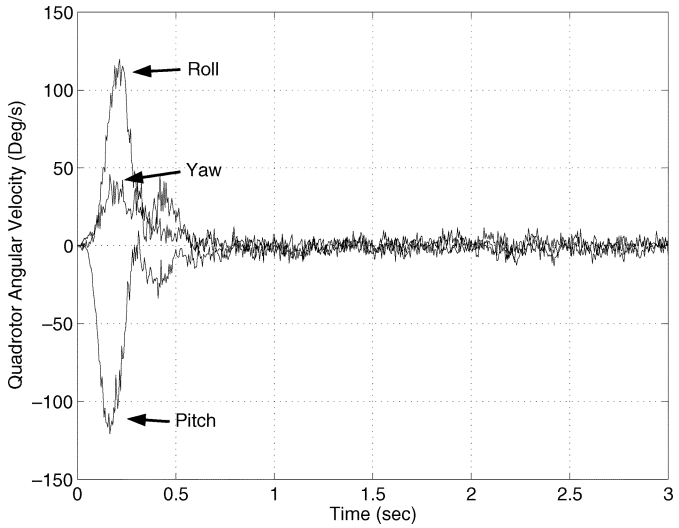

Fig. 5. Angular velocity, controller (13), Experiment 1.

from accelerometers. Configuring accelerometers[2] along the e_1 and the e_2 axes as tilt-meters and fusing this data with the

[2]A dual axis low-power device manufactured with microelectromechanical-system (MEMS) technology on a single integrated circuit (IC) weighs less than 1 g.

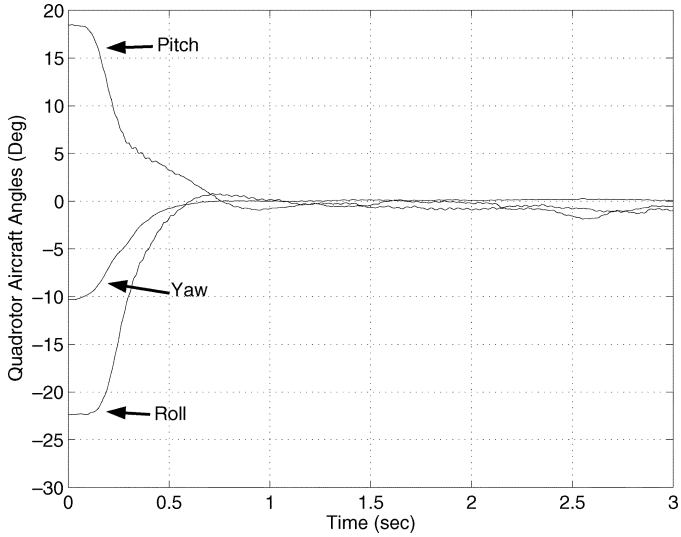

Fig. 6. Aircraft angles, controller (19), Experiment 1.

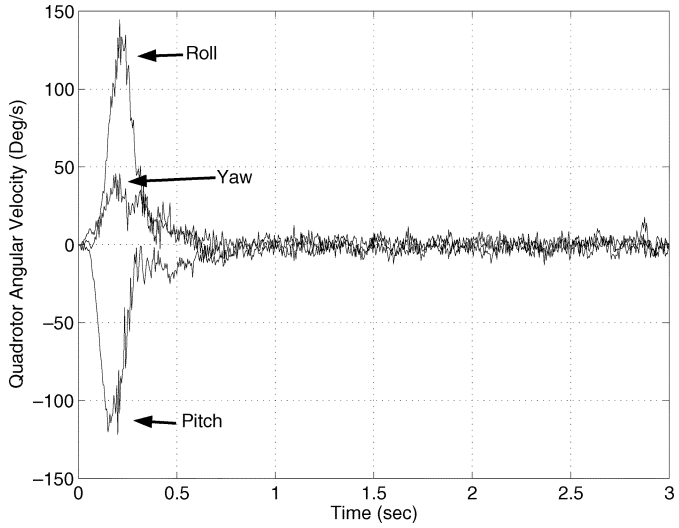

Fig. 7. Angular velocity, controller (19), Experiment 1.

measurements from the two gyroscopes mounted along the same axes by complementary filtering yields relatively accurate and drift free pitch and roll angle measurements [1]. Similar results are also possible for the yaw angle by fusing compass data with the yaw gyro signal, but have not been realized due to difficulties with compass readings.

In fact, the roll and pitch, for relatively small variations around the equilibrium point, are obtained through the fusion process, as follows $\bar{x} = G_t(s)[x_t] + G_g(s)[x_g]$, where $\bar{x}$ denotes (ϕ) or (θ). The signal x_t is obtained from the tilt-meter and x_g is obtained from the gyroscope. The transfer functions G_t and G_g are calculated such that the following equality is satisfied:

$$H_t(s)G_t(s) + sH_g(s)G_g(s) = 1 \tag{31}$$

where H_t and H_g denote the transfer functions describing the dynamics of the tilt-meter and the gyroscope, respectively.

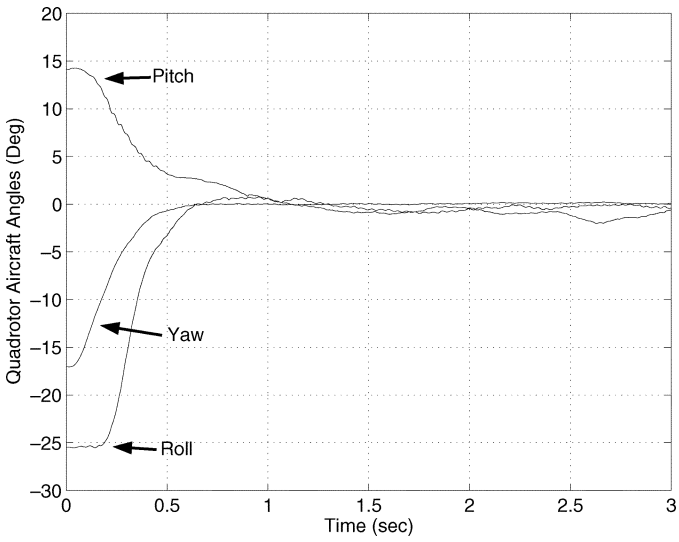

Fig. 8. Aircraft angles, controller (20), Experiment 1.

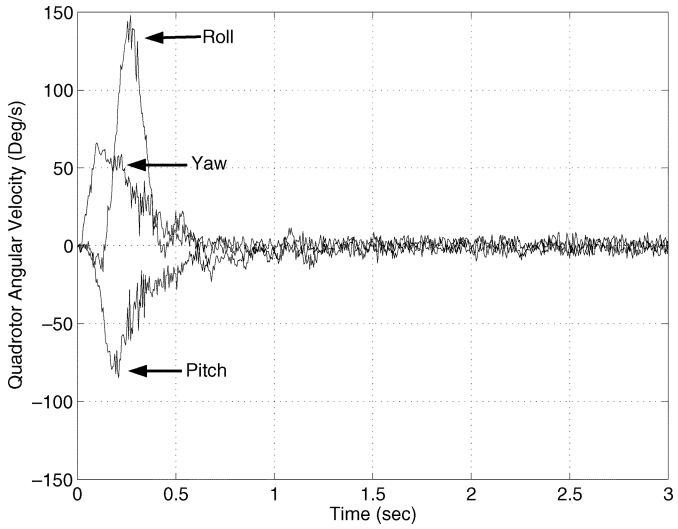

Fig. 9. Angular velocity, controller (20), Experiment 1.

Including the known dynamics for the tilt-meter, and assuming ideal dynamics for the gyroscope, we have

$$H_t(s) = \frac{1}{0.32s+1}, H_g(s) = 1. \tag{32}$$

Therefore, we can choose the filter-transfer functions as

$$G_t(s) = \frac{0.64s+1}{0.32s+1}, G_g(s) = \frac{0.1024s}{(0.32s+1)^2}. \tag{33}$$

The high-pass filter on the gyro branch effectively removes the low-frequency signal components at 40 dB per decade, sufficiently reducing the effects of drift at lower frequencies. Similarly, the low-pass filter on the tilt-meter branch effectively removes the high-frequency signal components at 20 dB per decade.

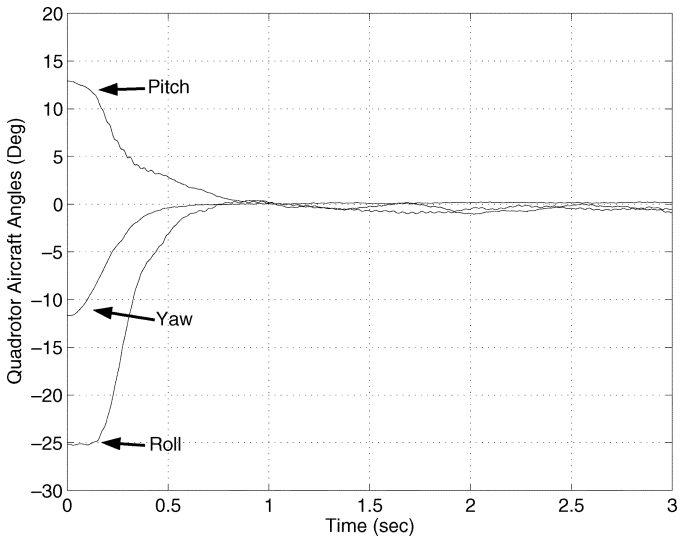

Fig. 10. Aircraft angles, controller (23), Experiment 1.

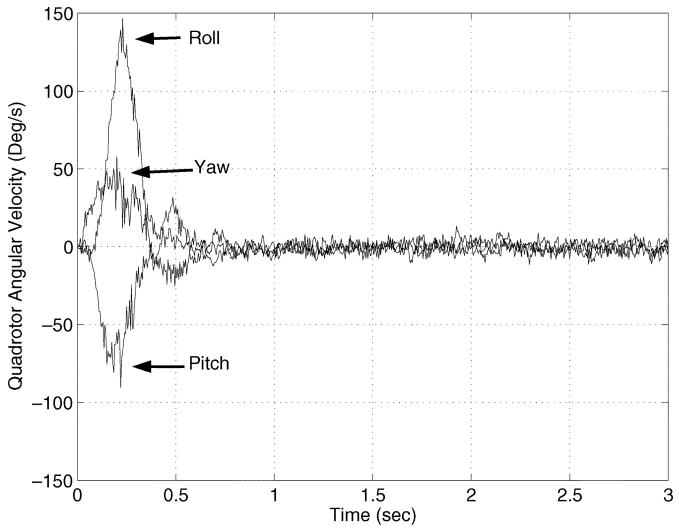

Fig. 11. Angular velocity, controller (23), Experiment 1.

In fact, the need for additional filtering has been observed and implemented on both the gyroscope and tilt-meter measurements to obtain a cleaner fused signal. The first-order low-pass filters have cutoff frequencies set at 20 Hz for the roll and pitch gyro signals, 10 Hz for the yaw gyro signal, and 2 Hz for the roll and pitch tilt-meter signals.

This type of angle estimation through complementary filtering has proven effective for relatively small roll and pitch aircraft angles. However, if we consider larger aircraft angles, this method will only give accurate estimates for individual planar rotations. More complex rotations of simultaneous roll, pitch and yaw angles require a nonlinear fusion technique as described in [14]. Due to the relative complexity and restrictions of this method and the fact that our experiments are controlled within restricted aircraft angles, we opted for the linear fusion method for the roll and pitch angles estimation.

The yaw angle estimation ψ, for relatively small variations around the equilibrium point, is obtained by $\psi = F_g(s)(1/s)[\dot{\psi}]$, where $\dot{\psi}$ denotes the measured angular rate from the yaw gyroscope and $F_g(s) = 1/(0.016s+1)$ is a

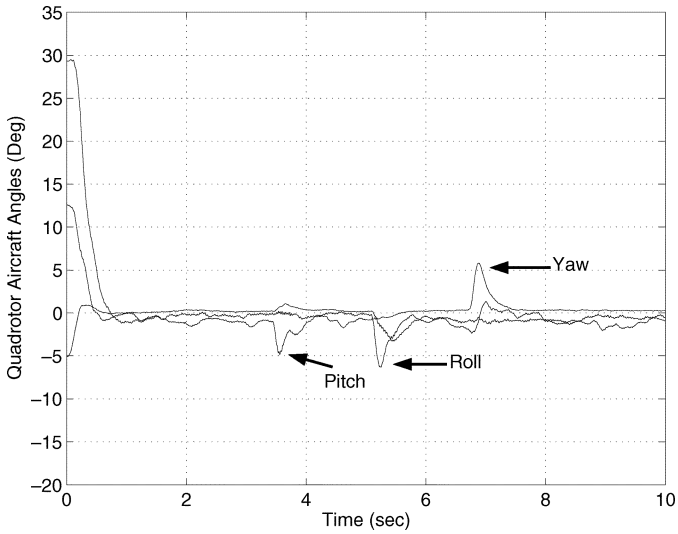

Fig. 12. Aircraft angles, controller (13), Experiment 2 (disturbance rejection).

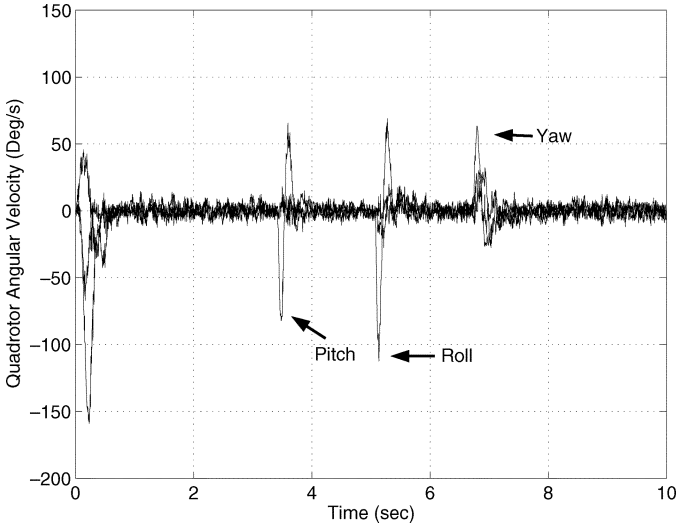

Fig. 13. Angular velocity, controller (13), Experiment 2 (disturbance rejection).

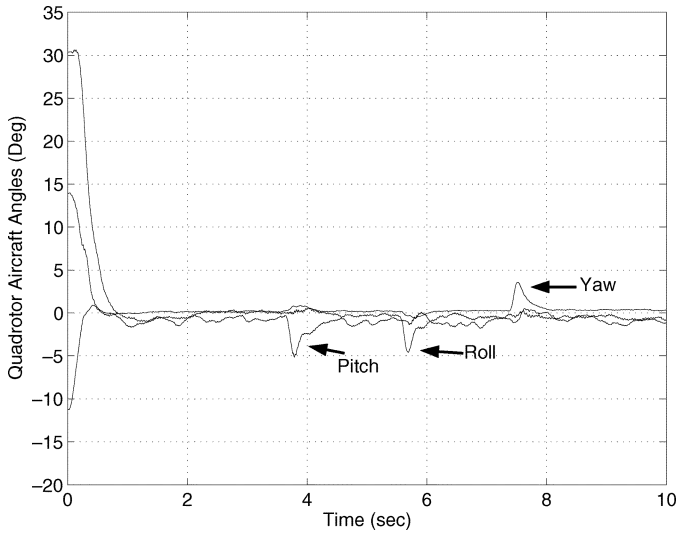

Fig. 14. Aircraft angles, controller (19), Experiment 2 (disturbance rejection).

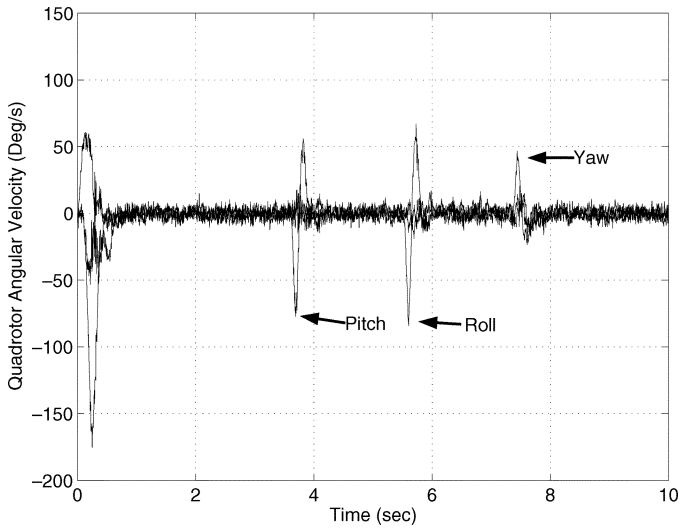

Fig. 15. Angular velocity, controller (19), Experiment 2 (disturbance rejection).

low-pass filter. The drift of the integrated yaw signal from the gyro alone has been noted and considered acceptable, and experimentation has continued without compensation for the yaw drift.

Once the Euler angles have been obtained, it is necessary to determine the equivalent Euler parameters, or quaternion representing this attitude. As shown in [18], this can be achieved as follows:

$$\begin{pmatrix} q_0 \\ q \end{pmatrix} = \begin{pmatrix} \cos\left(\frac{\phi}{2}\right)\cos\left(\frac{\theta}{2}\right)\cos\left(\frac{\psi}{2}\right) + \sin\left(\frac{\phi}{2}\right)\sin\left(\frac{\theta}{2}\right)\sin\left(\frac{\psi}{2}\right) \\ \sin\left(\frac{\phi}{2}\right)\cos\left(\frac{\theta}{2}\right)\cos\left(\frac{\psi}{2}\right) - \cos\left(\frac{\phi}{2}\right)\sin\left(\frac{\theta}{2}\right)\sin\left(\frac{\psi}{2}\right) \\ \cos\left(\frac{\phi}{2}\right)\sin\left(\frac{\theta}{2}\right)\cos\left(\frac{\psi}{2}\right) + \sin\left(\frac{\phi}{2}\right)\cos\left(\frac{\theta}{2}\right)\sin\left(\frac{\psi}{2}\right) \\ \cos\left(\frac{\phi}{2}\right)\cos\left(\frac{\theta}{2}\right)\sin\left(\frac{\psi}{2}\right) - \sin\left(\frac{\phi}{2}\right)\sin\left(\frac{\theta}{2}\right)\cos\left(\frac{\psi}{2}\right) \end{pmatrix}. \tag{34}$$

The quadrotor aircraft model parameters are given in Table I. I_{f_ϕ}, I_{f_θ}, and I_{f_ψ} denote the inertia of the airframe in the roll, pitch and yaw rotational directions (i.e., $I_f = diag(I_{f_\phi}, I_{f_\theta}, I_{f_\psi})$).

To explore the performance of each controller, three sets of experiments have been performed. Experiment 1 involves the aircraft attitude stabilization to zero starting from some initial configurations. In Experiment 2, we start the aircraft from an initial configuration and we stabilize its attitude to zero; thereafter, disturbances are introduced on the pitch, roll and yaw to explore the disturbance rejection performance. Both experiment 1 and 2 are performed for the control laws (13), (19), (20), and (23). Finally, Experiment 3 is performed only for the control law (13). It illustrates the attitude stabilization to the desired configuration ($\phi_d = -10°$, $\theta_d = 10°$, $\psi_d = -10°$), starting from some initial angles. As shown in Figs. 4–21, for the three experiments, we plotted the time-response of the yaw, pitch and roll in one graph and the three angular velocities in another graph.

Experiments on controllers (13) and (19) were performed with the following gains:

$\Gamma_1 = diag(240, 240, 60)$, $\Gamma_2 = 0.0025I$, and $\Gamma_3 = 4I$. Experiments on controllers (20) and (23) were performed with the following gains $\Gamma_4 = diag(0.5, 0.5, 0.2)$ and $\alpha = 4$. The

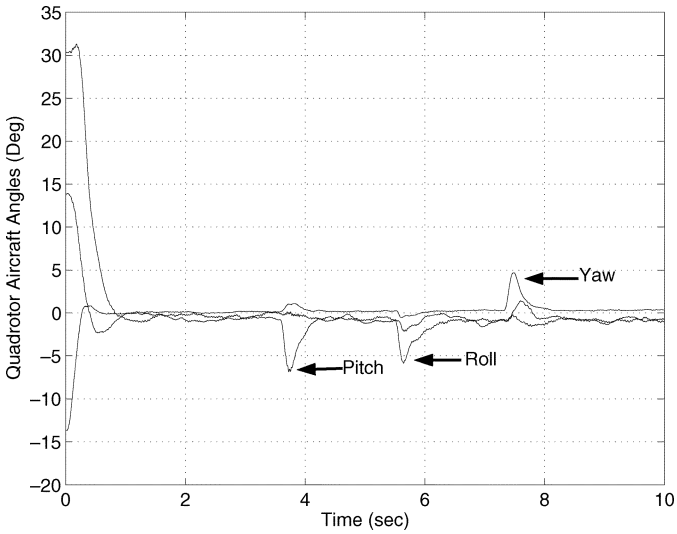

Fig. 16. Aircraft angles, controller (20), Experiment 2 (disturbance rejection).

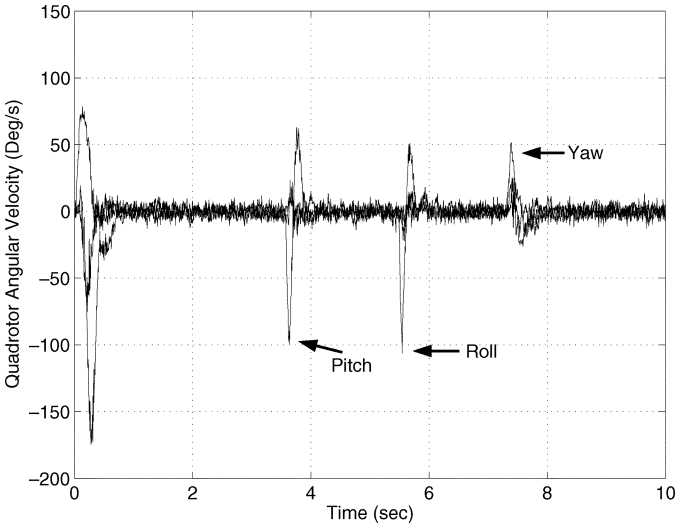

Fig. 17. Angular velocity, controller (20), Experiment 2 (disturbance rejection).

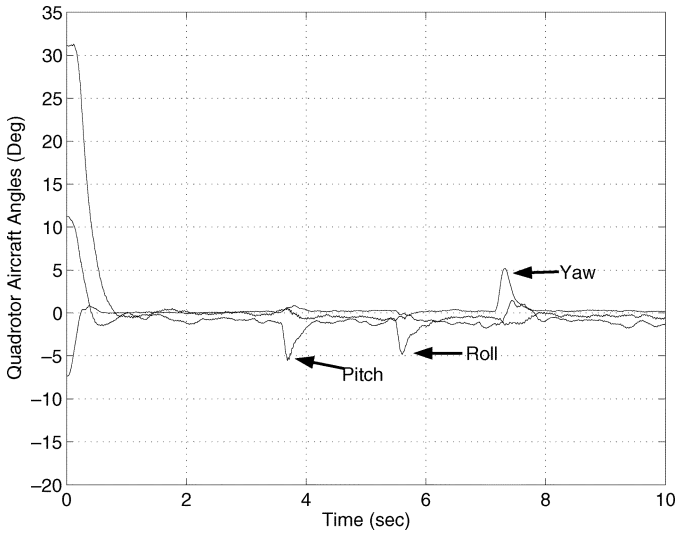

Fig. 18. Aircraft angles, controller (23), Experiment 2 (disturbance rejection).

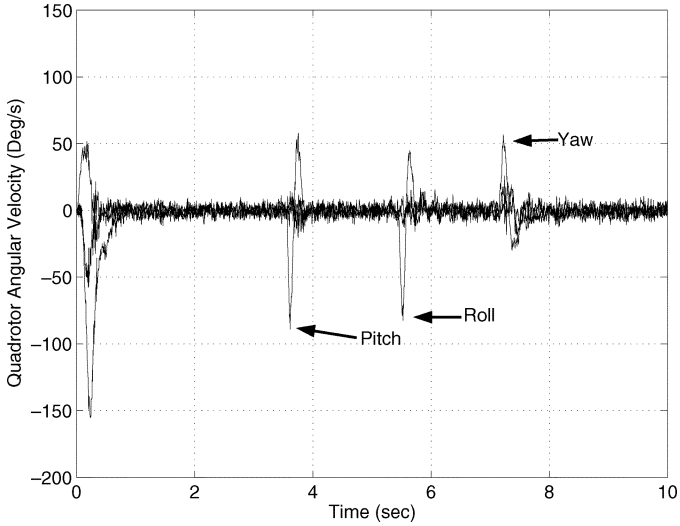

Fig. 19. Angular velocity, controller (23), Experiment 2 (disturbance rejection).

desired thrust and gain k_i remained the same throughout each experiment at $T = 1.5N$, $k_i = 0.002$, respectively, while the initial roll, pitch and yaw angles varied only slightly.

V. Conclusion

In this paper, it is shown that global exponential attitude stabilization can be achieved for the quadrotor aircraft. This result is based upon the compensation of the Coriolis and gyroscopic torques and the use of a PD^2 feedback structure, where the proportional action is in terms of the vector-quaternion and the two derivative actions are in terms of the airframe angular velocity and the vector-quaternion velocity. We also showed that the model-independent PD controller, where the proportional action is in terms of the vector-quaternion and the derivative action is in terms of the airframe angular velocity, without compensation of the Coriolis and gyroscopic torques, provides global asymptotic stability for our problem. The proposed controllers have been tested experimentally on a small-scale quadrotor aircraft equipped with "low-cost" sensors.

According to our experimental results (Figs. 4–21), the four controllers (13), (19), (20), and (23) provided quite similar results in terms of convergence and disturbance rejection. In fact, the compensation of the Coriolis and gyroscopic torques did not make much of a difference in our particular case due to the initial conditions and also to the relatively low speed. However, this will certainly make a difference in the case of large-angle maneuvers at high speed. Another important point that one should mention is the use of low-cost sensors for the attitude estimation as well as the linear fusion method used in our experiments. This was justified since our experimental setup was restricted to relatively small initial conditions. In fact, for large-angle maneuvers in the real world, more rigorous methods for the attitude estimation should be considered.

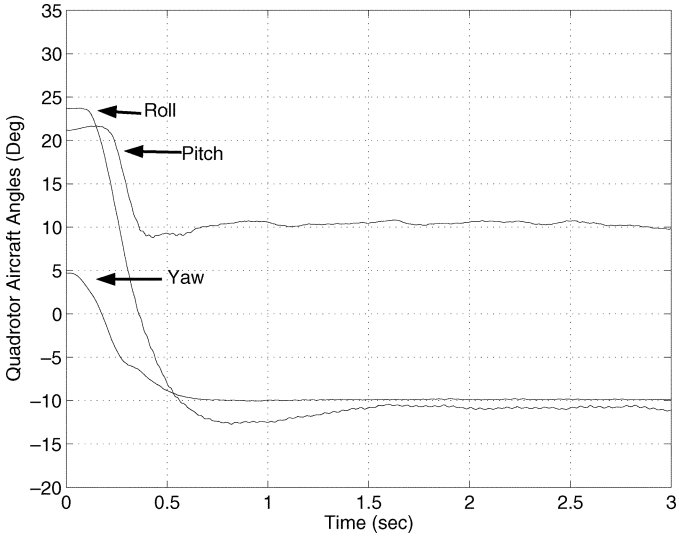

Fig. 20. Aircraft angles, controller (13), Experiment 3.

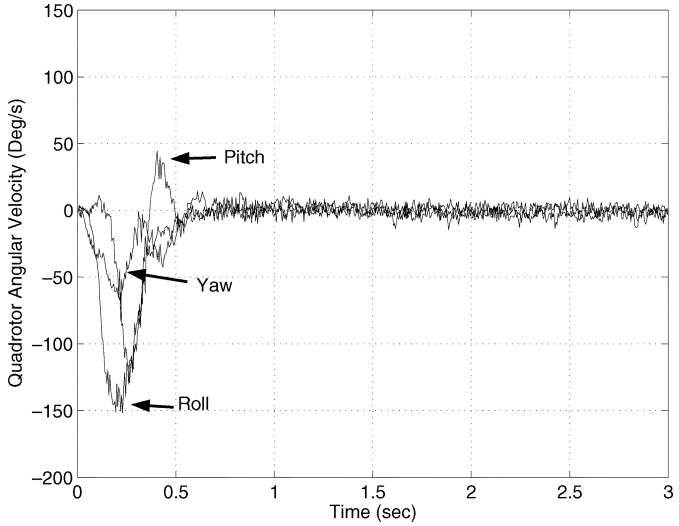

Fig. 21. Angular velocity, controller (13), Experiment 3.

ACKNOWLEDGMENT

The authors would like to thank K. Bhatia for building the ball joint base for the experiment, and the Associate Editor as well as the reviewers for their precious comments that helped us to improve the presentation of our results.

REFERENCES

[1] A. J. Baerveldt and R. Klang, "A low-cost and low-weight attitude estimation system for an autonomous helicopter," in *Proc. IEEE Int. Conf. Intelligent Engineering Systems*, 1997, pp. 391–395.

[2] P. Castillo, A. Dzul, and R. Lozano, "Real-time stabilization and tracking of a four rotor mini rotorcraft," *IEEE Trans. Control Syst. Technol.*, vol. 12, no. 4, pp. 510–516, Jul. 2004.

[3] O.-E. Fjellstad and T. I. Fossen, "Comments on 'The attitude control problem'," *IEEE Trans. Autom. Control*, vol. 39, no. 3, pp. 699–700, Mar. 1994.

[4] T. Hamel, R. Mahony, R. Lozano, and J. Ostrowski, "Dynamic modeling and configuration stabilization for an X4-flyer," in *Proc. IFAC World Congr.*, Barcelona, Spain, Jul. 2002.

[5] P. C. Hughes, *Spacecraft Attitude Dynamics*. New York: Wiley, 1986.

[6] B. P. Ickes, "A new method for performing control system attitude computation using quaternions," *AIAA J.*, vol. 8, pp. 13–17, 1970.

[7] S. M. Joshi, A. G. Kelkar, and J. T.-Y. Wen, "Robust attitude stabilization of spacecraft using nonlinear quaternion feedback," *IEEE Trans. Autom. Control*, vol. 40, no. 10, pp. 1800–1803, Oct. 1995.

[8] T. R. Kane, "Solution of kinematical differential equations for a rigid body," *J. Applied Mechanics*, pp. 109–113, 1973.

[9] A. R. Klumpp, "Singularity-free extraction of a quaternion from a direct-cosine matrix," *J. Spacecraft*, vol. 13, no. 12, pp. 754–755, 1976.

[10] F. Lizarraide and J. T. Wen, "Attitude control without angular velocity measurement: A passivity approach," *IEEE Trans. Autom. Control*, vol. 41, no. 3, pp. 468–472, Mar. 1996.

[11] R. Mahony and T. Hamel, "Adaptive compensation of aerodynamic effects during takeoff and landing manoeuvers for a scale model autonomous helicopter," *Eur. J. Control*, vol. 7, pp. 43–58, 2001.

[12] P. Pounds, R. Mahony, P. Hynes, and J. Roberts, "Design of a four-rotor aerial robot," in *Proc. Australian Conf. Robotics and Automation*, Auckland, Australia, 2002.

[13] R. W. Prouty, *Helicopter Performance, Stability and Control*. Melbourne, FL: Krieger, 1995.

[14] H. Rehbinder and X. Hu, "Nonlinear state estimation for rigid body motion with low-pass sensors," *Syst. Control Lett.*, vol. 40, no. 3, pp. 183–190, 2000.

[15] M. W. Spong and M. Vidyasagar, *Robot Dynamics and Control*. New York: Wiley, 1989.

[16] A. Tayebi and S. McGilvray, "Attitude stabilization of a four-rotor aerial robot," in *Proc. 43rd IEEE Conf. Decision and Control*, Atlantis, Bahamas, Dec. 2004, pp. 1216–1221.

[17] J. T.-Y. Wen and K. Kreutz-Delgado, "The attitude control problem," *IEEE Trans. Autom. Control*, vol. 36, no. 10, pp. 1148–1162, Oct. 1991.

[18] J. R. Wertz, *Spacecraft Attitude Determination and Control*. Amsterdam, The Netherlands: D. Reidel, 1978, Members of the Technical Staff, Attitude Systems Operation, Computer Sciences Corp..

[19] B. Wie, H. Weiss, and A. Arapostathis, "Quaternion feedback regulator for spacecraft eigenaxis rotations," *AIAA J. Guid. Control*, vol. 12, no. 3, pp. 375–380, 1989.